The Effect of Transient Power Ramp-Up on Structural and Optical Properties of CuO Thin Films Prepared by Radio Frequency Magnetron Sputtering

10 authors, including:

Cyril C.F. Kumachang
Pennsylvania State University
2 PUBLICATIONS   0 CITATIONS

SEE PROFILE

Dahiru Muhammad Sanni
African University of Science and Technology
25 PUBLICATIONS   198 CITATIONS

SEE PROFILE

Yusuf Afolabi Olanrewaju
North Carolina State University
11 PUBLICATIONS   63 CITATIONS

SEE PROFILE

Nicole Doumit
Institut Supérieur d'Electronique de Paris
19 PUBLICATIONS   39 CITATIONS

SEE PROFILE

RESEARCH ARTICLE

ADVANCED
ENERGY & SUSTAINABILITY
RESEARCH
Open Access
www.advenergysustres.com

The Effect of Transient Power Ramp-Up on Structural and Optical Properties of CuO Thin Films Prepared by Radio Frequency Magnetron Sputtering

Cyril C. F. Kumachang, Daniel I. Amune, Ivy M. Asuo, Dahiru Sanni, Yusuf A. Olanrewaju, Nicole Doumit, Richard Koech, Vitalis Anye, Esidor Ntsoenzok, and Nutifafa Y. Doumon*

Transition metal oxides have found application as charge transport materials (CTMs) in perovskite solar cell devices due to their better environmental stability and superior electronic properties compared to organic CTMs. Many researchers have used radio frequency (RF) magnetron sputtering to deposit inorganic CTMs on inorganic layers. However, such efforts on perovskites have been limited by the distortion of high-energy ions of the sputtering gas energized by the RF power and temperature. The ions may also distort the interface between transparent conducting oxides and the charge transport layers, thereby increasing optical scattering. Thus, the effect of ramp power during RF magnetron sputtering deposition on the structural and optical properties of copper oxide thin films is investigated. While the optical transmittance of the films decreases with increased RF power, it remains the same for all ramped power films; however, it has a similar profile as the highest RF power film. As the ramp power increases, the X-ray diffraction shows that the films become more polycrystalline with a monoclinic crystal structure. The energy-dispersive X-ray spectroscopy results reveal that the atomic concentration of copper slightly increases with the RF power, whereas oxygen concentration slightly decreases.

1. Introduction

The search for better techniques and materials for efficient and stable perovskite optoelectronic and photovoltaic devices has resulted in the development of oxide materials based on transition metals for use as the charge transport layer and transparent conducting oxides in perovskite solar cell fabrication. The preparation of thin metal oxide films has been achieved using several methods.[1] These methods include 1) chemical solution deposition[2,3] such as sol–gel method,[4–7] spray pyrolysis[6] metal–organic decomposition, chelation, polymer-assisted deposition, and hydrothermal methods; 2) Physical vapor deposition[2] such as sputtering,[8–14] evaporation,[15] and molecular beam epitaxy;[2] and 3) chemical vapor deposition (CVD) including atomic layer deposition, atmospheric pressure CVD, plasma-enhanced CVD, and so on. Sputter deposition is a mature method widely used in the electronics industry to deposit thin films. Many researchers have used this technique to deposit thin films of electron transport materials,

C. C. F. Kumachang, I. M. Asuo, N. Y. Doumon
Department of Materials Science and Engineering
The Pennsylvania State University
University Park, PA 16802, USA
E-mail: nzd5349@psu.edu

D. I. Amune, Y. A. Olanrewaju, R. Koech, V. Anye, E. Ntsoenzok
Department of Materials Science and Engineering
African University of Science and Technology
KM 10 Airport Road, Galadimawa, P. M.B. 681, Garki, Abuja, Federal
Capital Territory, Nigeria

The ORCID identification number(s) for the author(s) of this article can be found under https://doi.org/10.1002/aesr.202300258.

I. M. Asuo, N. Y. Doumon
Alliance for Education, Science, Engineering, and Design with Africa
The Pennsylvania State University
University Park, PA 16802, USA

D. Sanni
Department of Physics
Nile University of Nigeria
Plot 681, Cadastral Zone C-OO, Research & Institution Area Nigeria,
Airport Rd, Jabi, Abuja 900001, Nigeria

N. Doumit
LISITE Laboratory
ISEP
10 Rue de Vanves, 92130 Issy-les-Moulineaux, France

R. Koech
Department of Mathematics, Physics, and Computing
Moi University
P.O. Box 3900-30100, Eldoret, Kenya

**ADVANCED
SCIENCE NEWS**

www.advancedsciencenews.com

**ADVANCED
ENERGY & SUSTAINABILITY
RESEARCH**
Open Access

www.advenergysustres.com

hole transport materials, and even perovskite absorbers.[16] It has also been used to deposit electron transport material directly on the perovskite absorber.[17] This technique has the advantage of low-temperature deposition, making it suitable for flexible device fabrication. It is also used to deposit thin films free of uncontrolled impurities due to the high vacuum process. Furthermore, the properties of the films can be easily and repeatedly tuned due to well-controlled deposition parameters.

Due to the hygroscopic nature of additive salt used to increase the conductivity of organic hole transport materials in perovskite solar cells, there is a continuous quest to fabricate highly stable perovskite solar cells. Thus, researchers are considering fabricating perovskite solar cells using inorganic materials, as they have been reported to be more stable than their organic counterparts. However, most solvents used in depositing inorganic charge transport layers partly wash off the perovskite layer.[17] Subbiah et al. have utilized the radio frequency (RF) magnetron sputtering technique to deposit a zinc oxide charge transport layer (CTL) atop a formamidinium lead bromide absorber layer.[17] However, the high-energy gas ions tend to damage the structure of the underlying perovskite surface, leading to poor efficiency. The destruction may be attributed to the initial high-energy ions arriving at the surface of the layer, energized by relatively high RF power. Moreover, distortion of the interface between TCO and CTL may also be attributed to these high-energy ions, leading to increased optical scattering. Therefore, optimizing the interface between the TCO and CTL is pertinent to improving the optical properties of these layers. Thus, we investigate the effect of RF power ramp on the structural and optical properties of copper oxide (CuO) thin films. While the compositional grading during RF magnetron sputtering has been investigated,[18] to the best of our knowledge, there is no report on the effect of power ramp on the structure and properties of CuO thin films. Thus, in this article, we studied the effect of ramp power during RF magnetron sputtering deposition on the structural and optical properties of CuO thin films for possibly perovskite solar cell applications.

2. Results and Discussion

The schematic of the power ramp procedure and pictures of all deposited CuO films are shown in Figure S1 and S2, Supporting Information, respectively. For samples deposited at 60, 80, 100, and 120 W, we observed a transition from a light brown color for the 60 W deposited films to a darkish color for the 120 W deposited films, suggesting an increase in CuO films density and

V. Anye
Faculty of Engineering
Nile University of Nigeria
Plot 681, Cadastral Zone C-OO, Research & Institution Area Nigeria, Airport Rd, Jabi, Abuja 900001, Nigeria

E. Ntsoenzok
CEMHTI-CNRS
Site Cyclotron, 3A Rue de la Férollerie, 45071 Orléans, France

N. Y. Doumon
Materials Research Institute
The Pennsylvania State University
University Park, PA 16802, USA

thickness. However, all ramped-up power films show a similar dark color, indicating that this set of films may exhibit similar density and physical properties. The thicknesses of the films were determined using cross-sectional scanning electron microscopy (SEM) imaging as shown in Figure S3c, Supporting Information, obtained from the SEM cross-sectional images and Bruker DektakXT Stylus profilometer. The measured average thicknesses for the ungraded films with RF power 60, 80, 100, and 120 W were found to be 67.8 ± 4.2, 83.1 ± 3.9, 101.3 ± 5.7, and 192 ± 8 nm, respectively, in agreement with the change in color observed in Figure S2, Supporting Information. While the thicknesses for the graded films with RF power were similar to or higher than the ungraded CuO films deposited at 120 W, they recorded average thicknesses of 178.6 ± 3.2, 233.7 ± 7.2, 198 ± 12, and 234.1 ± 3.3 nm, respectively.

The structural properties and morphology of the films were studied using X-ray diffraction (XRD), SEM, and energy-dispersive X-ray spectroscopy (EDS). The crystallographic structure was studied using the Malvern Panalytical Empyrean III X-ray diffractometer with Cu Kα ($k = 1.5418$ Å) radiation for 2θ values in the 20–70 degrees range. The XRD patterns of the CuO thin films deposited under different RF powers and ramped powers are shown in **Figure 1**. The peaks at 2-theta 34.8° and 37.5° are attributed to the $(\bar{1}11)$ and (111) planes, respectively, of monoclinic crystal family of CuO according to the Joint Committee for Powder Diffraction Standards (JCPDS file no. 01-089-2531) data for CuO, thus indicating a monoclinic structure of the deposited CuO thin films with preferred $(\bar{1}11)$ and (111) crystallographic orientations, as also observed in ref. [19]. The results reveal that as the RF power increases, there is an enhancement of the polycrystalline structure, with the polycrystalline films having a monoclinic crystal structure with the main CuO $(\bar{1}11)$ and (111) orientations[20] with higher intensity of the diffraction peaks at approximately 34.8° and 37.5°.

Figure 2a shows the full width half maximum (FWHM) of the CuO $(\bar{1}11)$ diffraction peaks at 60, 80, 100, and 120 W with values of 0.288°, 0.276°, 0.271°, and 0.579°, respectively (see Table S1, Supporting Information). These results indicate that increased RF power enhanced the intensity of the crystalline phase. Thus, with more crystalline area under the curve, the increase in RF power resulted in increased crystallinity. The observed effect of increased RF power is insignificant during ramping up power, as shown in Figure 2b and Table S2, Supporting Information, where the FWHM of the ramped RF power R_1, R_5, R_10, and R_20 W deposited films are found to be in the same range and similar to that of the film deposited at 120 W. The obtained FWHM values are 0.480°, 0.506°, 0.449°, and 0.509°. This means that the ramped samples indicate overall better crystallinity. However, increasing sputtering power as the deposition progresses can increase the variation in energy of sputtered atoms. This leads to an increased interruption in the arrangements of the sputtered atoms. This effect is more significant at a higher power ramp rate, as observed in Figure 2b. While all the ramped films show a small peak (110) at around 2-theta 32.5° compared to the absolute power deposited films, the films at 20 W power ramp show an extra mild peak (220) at around 2-theta 68°. Thus, power ramping during the sputter
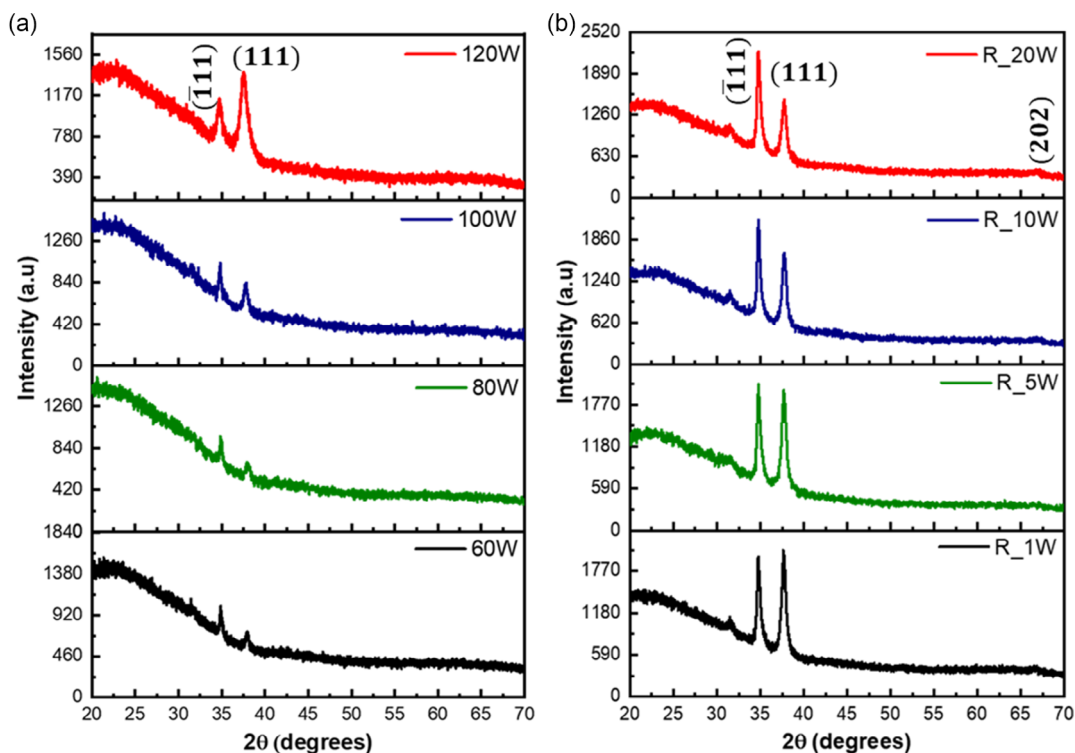
Figure 1. XRD diffraction pattern of CuO thin films deposited by RF magnetron sputtering a) without power ramp and b) with power ramp.
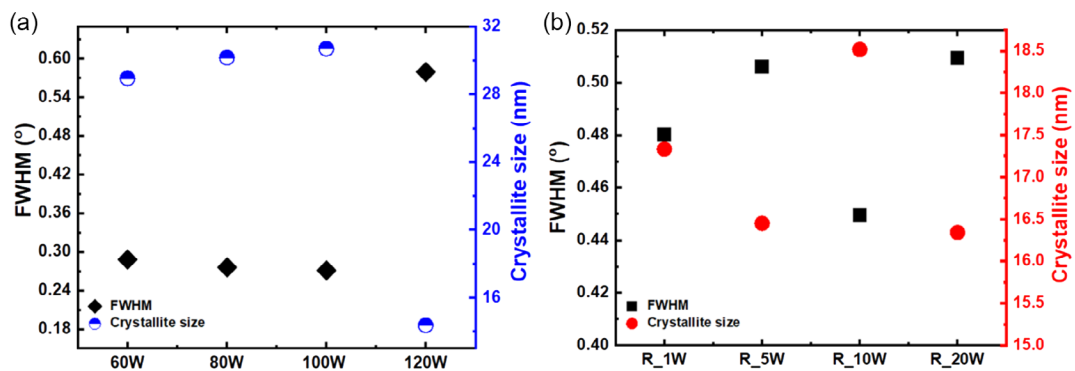

Figure 2. Crystallite sizes and the FWHM values of the CuO deposited thin films a) without power ramp (Blue and Black colors respectively) and b) with power ramp (red and black colors, respectively).

deposition can be used as a tool to control the crystallinity of the deposited film.

It is possible to control the structure of films deposited by controlling the deposition techniques. This agrees with previous reports on inorganic films deposited using RF sputtering. Crystalline film formation typically requires high-temperature annealing. However, from the XRD results in Figure 1, we found that a ramped RF power room temperature deposition technique can provide an alternative to high-temperature crystalline film formation.

The crystallite sizes of the films are shown in Figure 2, Table S1 and S2, Supporting Information. The crystallite sizes

were obtained by considering the most intense peaks and using the Scherrer equation:[21]

$$D = K \frac{\lambda}{\beta \cos\theta} \tag{1}$$

where λ is the wavelength of the X-ray radiation, K is a constant taken as 0.9, θ is the diffraction angle, and β is the FWHM. We observed an increased average grain/crystallite size with increased Cu incorporation for RF power from 60 to 100 W RF power with a decrease at 120 W. A similar observation was made by Ajee et al.[22] for increased temperature of CuO thin

film. We attributed this increase to probable combined effects of increased Cu atoms, increased growth rate, and reorientation. This agrees with the EDS results shown in Figure 4. It has been reported that an increase in grain/crystal size is associated with increased RF power due to the high kinetic energy of sputtered atoms arriving on a substrate from a sputtering target and enhanced nuclear growth.[23]

To investigate the nanostructure surface morphology of the CuO films, we used the Zeiss Gemini 500 (G500) field emission scanning electron microscope (FE-SEM) to image the CuO films. **Figure 3** shows the 200 nm scale SEM images with the red and blue panels highlighting the films deposited without and with power ramping, respectively. Similar images for the films taken at 1 μm scale are shown in Figure S4, Supporting Information. Compared to the SEM image of bare glass in Figure S3a,b, Supporting Information, a homogenous CuO grain size distribution is seen in the micrographs. We can observe a fully consistent uniform surface coverage of the glass with more compact CuO films in full contact with the glass substrate, as seen in the cross-sectional image in Figure S3c, Supporting Information. The granular nature of the films confirms the polycrystalline nature of the CuO films, as predicted by the XRD results. The deposited films with power ramping in Figure 3 (blue panel) appear to have the same denser and smaller CuO crystal grains similar to the dense 120 W deposited films, and a better surface morphology coverage in contrast to the images of the 60, 80, and 100 W deposited CuO films in Figure 3 (red panel). The power ramp deposition films exhibited similar roughness with an average root-mean-square roughness, r_{ms} of 0.7 ± 0.1 nm compared to 0.5 ± 0.1 nm for the rest of the films. This assertion is very noticeable when the 60 and 120 W micrographs are compared. Indeed, this agrees with the XRD results suggesting that the crystallinity and grain growth of CuO films on glass substrate strongly depends on the deposition technique and RF power.

To understand the elemental composition and distribution of the films on the glass substrate, an Oxford UltimMax 100 sensor configured on the SEM instrument was used for EDS measurement. The EDS spectra in **Figure 4** confirm that our film was majorly made up of Cu and O. Table S3–S6, Supporting Information, show the atomic and weight percentages of the constituent elements. The copper and oxygen peaks confirm the formation of CuO in agreement with the XRD results, whereas the sharp peaks related to Cu and O confirm the significant CuO loading at the surface of the glass substrate. EDS mapping revealed a good degree of homogeneity in the distribution of the different elements of the thin film on the glass, as shown in Figure S5 and S6, Supporting Information. Notwithstanding defect chemistry of nonstoichiometric compounds and solid solutions should be determined through careful measurements of lattice constants, densities, and conductivity dependence on atmosphere, Ohya et al.[24] speculated that as oxide crystals usually cannot accommodate a large interstitial oxide ion, the nonstoichiometric of p-type CuO is expected to be cation deficient for doped CuO. The defects equation is shown as follows:[24]

$$2CuO + \frac{1}{2}O_2 \leftrightarrows 2Cu'_{Cu} + V''_{Cu} + 3O_O \tag{2}$$

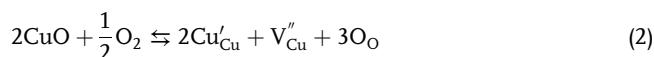$$Cu'_{Cu} \leftrightarrows 2Cu^X_{Cu} + P' \tag{3}$$

Figure 4a,b shows that as the RF power increases, the atomic concentration of the copper increases from 46% to 48%. The percentage of oxygen atoms reduced as RF increased to 120 W from 54% to 52%. These could be related to the knocking-off of copper atoms from their lattice position, which created copper vacancies responsible for the p-type character of CuO. Researchers have reported that the CuO deposition procedures and postdeposition treatment can result in a transition in the material conductivity from p- to n-type due to oxygen vacancies introduced at high temperatures.[25,26] Researchers have made many attempts to convert CuO, a well-known p-type semiconductor, into an n-type semiconductor, including doping and annealing.[26] In Figure 4b, the reduction in the peak intensity at 0.5 KeV indicates oxygen depletion at higher RF power, thus suggesting a possible transition from p- to n-type conductivity of CuO.[26] This is a subject for further investigation. Depending on the deposition procedures, CuO can possess combined n- and p-type semiconducting characteristics, and the conductivity can change from p- to n-type.[27] This property is undesirable in solar cell applications as it could increase charge carrier recombination.[28]
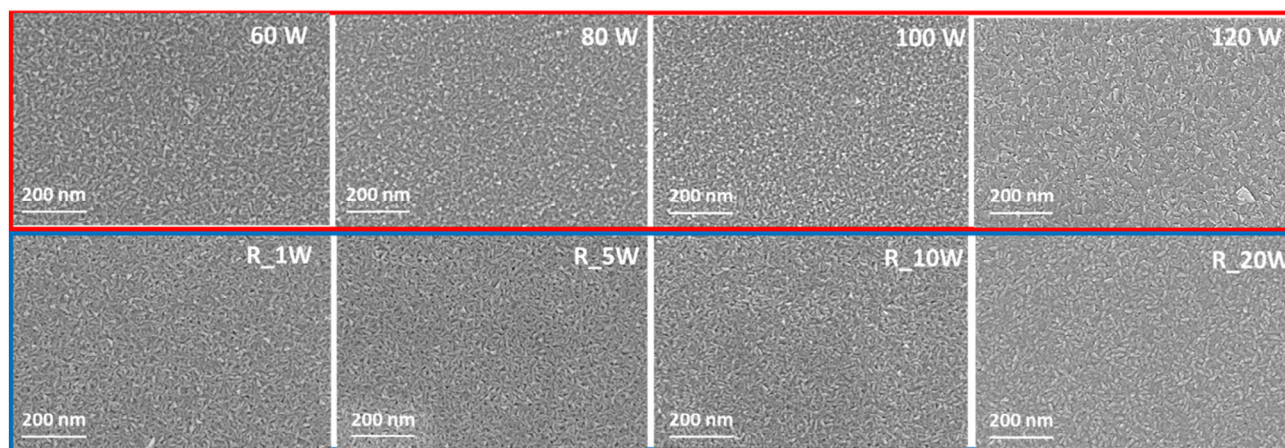

Figure 3. SEM Images of CuO thin films deposited by RF magnetron sputtering without power ramp (red panel) and with power ramp (blue panel) taken at 200 nm magnification.
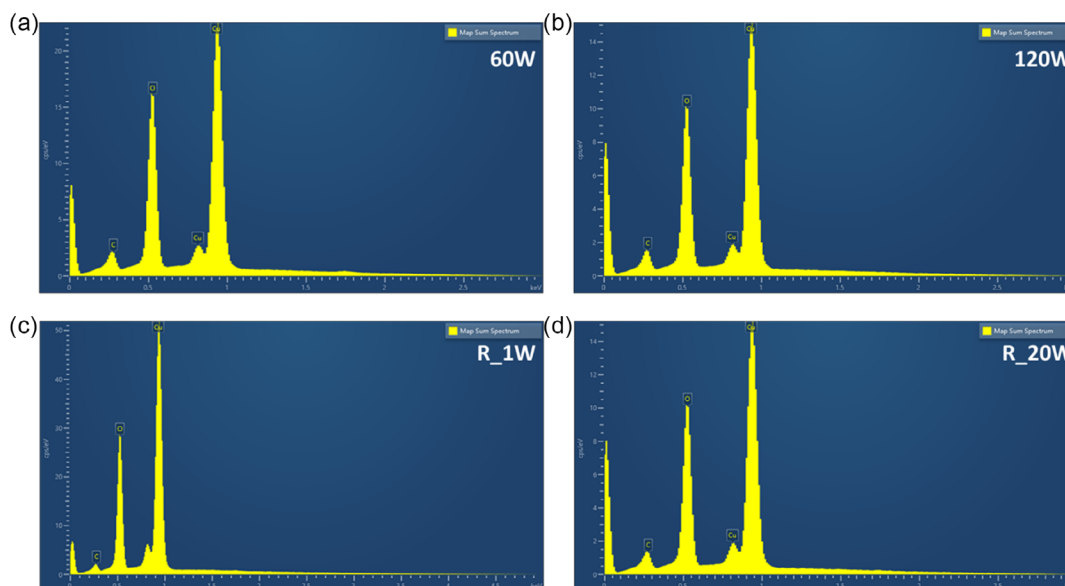
Figure 4. EDS pattern of CuO thin films deposited without power ramp: a) at 60 W and b) at 120 W; and with a power ramp: c) at R_1W and d) at R_20 W.

The EDS spectra for the ramping method in Figure 4c,d appear to be a similar trend, but minute changes in the atomic concentration of the copper (increase from 47% to 48%) and oxygen (reduction from 53% to 52%) concentration. This suggests that with the ramping method of deposition, we can achieve almost negligible to no change in the atomic concentration of Cu and O in the CuO films, regardless of the thickness of the deposited films.

Next, we investigated the optical properties of the deposited CuO thin films using the PerkinElmer UV/vis/NIR Lambda 1050 + Spectrometer. As shown in **Figure 5**a, the transmittance decreases with increased RF power, with a significant decrease observed for the 120 W films across the whole spectrum. However, in Figure 5b, the graded samples show perfect overlaps of the transmittance as the wavelength increases from UV through the visible region with a slight difference in the infrared region. This phenomenon is not observed in the transmittance spectra of films deposited without power grading.

UV radiation could cause oxygen vacancies and defects in the perovskite crystals, breaking the device down. Perovskite films have an intense absorption range in the UV region (200–400 nm).[29] As shown in Figure 5a,b, though the UV transparency of the films is relatively low, it decreases more at a higher RF power and ramped powers. Thus, UV filtering can be improved by depositing the CuO films at a higher power or via ramped power, hence enhancing the stability of the perovskite solar cell. This result is also important for applications such as UV light sensors and lighting, where their high UV transmittance demonstrates the highest quality materials on glasses. Additionally, UV coating on clear lenses can effectively block UV light, thereby offering protection to the eye. Thus, by depositing thin films at a higher power ramp, one can achieve improved UV-blocking efficiency of lenses.

For device application, the CuO thin film thickness and UV absorption become critical for performance in terms of efficiency

and stability. While high RF power and ramped power favors CuO as CTL due to their low transmittance in the UV, the control of the film thickness is of interest. We deposited a CuO film at 60 W and 4.7×10^{-3} mbar for 1000 s and obtained a 12.5 nm thickness. Sangwaranatee et al. showed that varying chamber pressure during the sputtering deposition significantly impacts film thickness with higher pressure, yielding low thicknesses.[30] We believe that combining pressure difference, ramp power, and duration of deposition would help control thickness for device application.

The transmittance data was later used to determine the value of the optical bandgap. The relationship between the absorption coefficient (α) and the incident photon energy ($h\nu$) can be written as follows:

$$(\alpha h\nu) = A(h\nu - E_g)^n \tag{4}$$

where A is a constant.

For a direct bandgap material such as CuO, the value of n is 2. The bandgap estimated for the graded and ungraded samples ranges between 2.3 and 2.83 eV, as shown in Figures 5a,b. For the ungraded films in Figure 5a, under RF power conditions of 60, 80, 100, and 120 W, the energy bandgap E_g was 2.80, 2.83, 2.80, and 2.27 eV, respectively. In Figure 5b, for films at ramp power of 1, 5, 10, and 20 W, the energy bandgap E_g was 2.30, 2.57, 2.64, and 2.71 eV, respectively. Also, copper is multivalent, thus forming several oxides (i.e., CuO and Cu$_2$O). Accordingly, the bandgap of CuO semiconductors varies with the phases present, deposition procedures, and postdeposition treatment.[26,31] In brief, depending on the phases, fabrication procedure, and postdeposition treatment, the bandgap reported for different CuO semiconductors ranges from 1.4 to −3.19 eV,[26,27,31–35] which places the obtained E_g in the acceptable range seen in the literature.
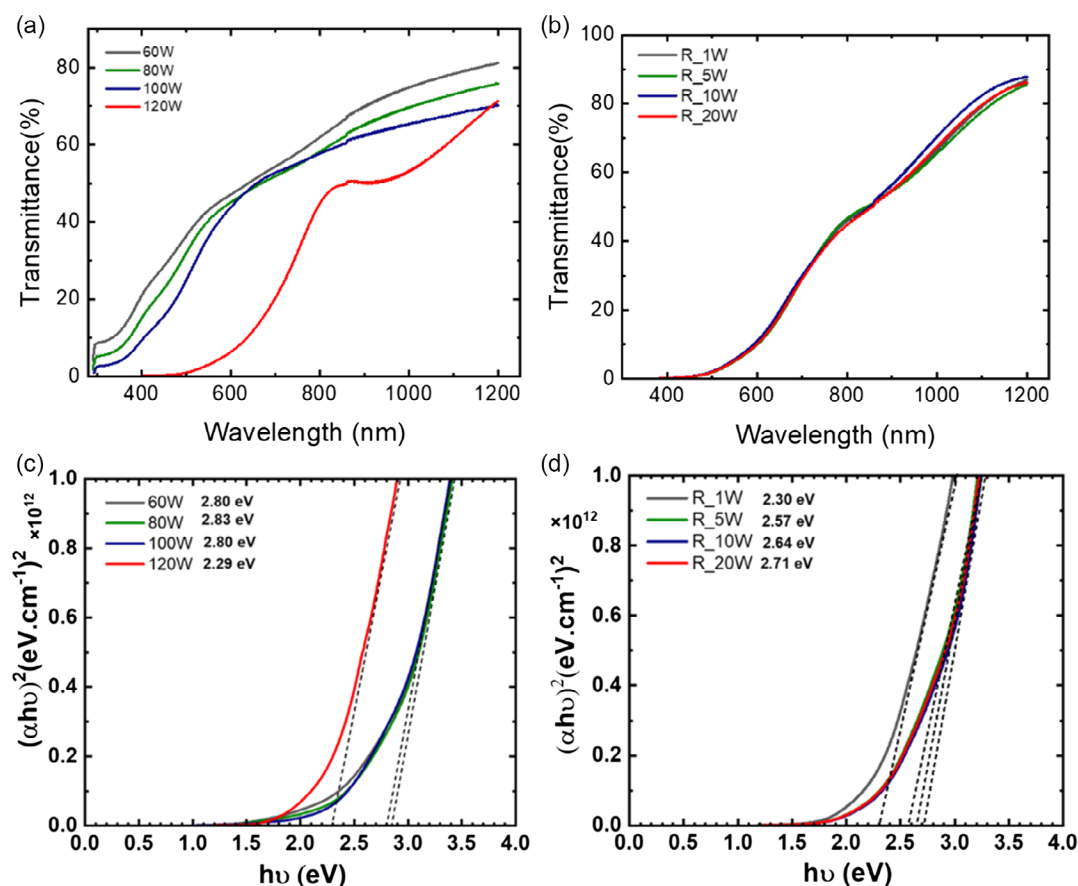
Figure 5. UV–vis measurement of the CuO thin films. Optical transmittances of deposited films a) without RF power ramp and b) with RF power ramp. Direct bandgaps of the deposited films c) without RF power ramp and d) with RF power ramp.

3. Conclusion

We successfully deposited thin films of CuO with varying deposition parameters by RF magnetron sputtering. In agreement with previous reports, the deposition rate increases with ramp time and RF power. The XRD results revealed that the films deposited are polycrystalline. The optimum deposition condition for application in solar cells that gives a good blend of XRD, SEM, and transmittance quality is the ramp step or graded RF power samples. However, further thickness control is needed for using CuO films as a CTL in photovoltaic cells. These results also provide an additional understanding of the critical role of RF power during the sputtering of thin films compared to normal RF power deposition. The results also suggest the possibility of CuO conductivity due to oxygen depletion, which would need to be confirmed via further experiments.

4. Experimental Section

The CuO thin films were deposited using a single gun Kurt J Lesker CMS-18 RF magnetron sputtering system. Atoms were sputtered from a CuO target (diameter = 76 mm) onto a glass substrate at a standard frequency of RF, 13.56 MHz. The distance between the target and the substrate was about 120 mm. The chamber pressure in the deposition process was maintained at 4.7×10^{-3} mbar. Argon gas was used as the working

gas for the sputtering process, and the flow rate was kept at 11.2 sccm while rotating the samples at 10 rpm throughout the deposition. These depositions were carried out at room temperature, 20 °C, crucial for the CTL deposition if atop of perovskite active layer.

First, we deposited CuO thin films at 60 W for 60 min at a gas flow rate of 11.2 sccm. The same steps were followed for depositions at 80, 100, and 120 W. Next, we also deposited the thin films with ramping power from 60 to 120 W in steps of 1 W at 59 s intervals for a total deposition time of 60 min. Similarly, we prepared samples with power ramped up from 60 to 120 W in steps of 5 W at 277 s intervals for a total deposition time of 60 min. The third and fourth sets of samples were deposited with ramped power of 10 W at 514 s intervals and in steps of 20 W at 900 s intervals, respectively, from 60 to 120 W.

The physical and structural characteristics of the samples were obtained using 1) Malvern Panalytical Empyrean III X-ray diffractometer for the crystallinity of the film; 2) Zeiss Gemini 500 (G500) FE-SEM for nanostructure morphology imaging and thickness confirmation via SEM cross-sectional imaging; 3) Oxford UltimMax 100 sensor configured on the SEM instrument for elemental composition and distribution in the films; and 4) PerkinElmer UV/vis/NIR Spectrometer Lambda 1050+ for optical properties of the films.

Supporting Information

Supporting Information is available from the Wiley Online Library or from the author.

Acknowledgements

Conflict of Interest

The authors declare no conflict of interest.

Data Availability Statement

The data that support the findings of this study are available from the corresponding author upon reasonable request.

Keywords

[1] G. Papadimitropoulos, N. Vourdas, V. E. Vamvakas, D. Davazoglou, *Thin Solid Films* **2006**, *515*, 2428.

[2] K. Wasa, *Thin Film Technologies for Manufacturing Piezoelectric Materials*, Science and Technology, Woodhead Publishing Limited **2010**, pp. 481–532.

[3] L. Fei, M. Naeemi, G. Zou, H. Luo, *Chem. Rec.* **2013**, *13*, 85.

[4] M. Jlassi, I. Sta, M. Hajji, H. Ezzaouia, *Mater. Sci. Semicond. Process.* **2014**, *21*, 7.

[5] T. Chtouki, L. Soumahoro, B. Kulyk, H. Erguig, B. Elidrissi, B. Sahraoui, *Optik* **2017**, *136*, 237.

[6] R. A. Ismail, S. Ghafori, G. A. Kadhim, *Appl. Nanosci.* **2013**, *3*, 509.

[7] S. Belhamri, N. E. Hamdadou, *Surf. Rev. Lett.* **2018**, *25*, 1.

[8] T. S. Sathiaraj, *Microelectron. J.* **2008**, *39*, 1444.

[9] J. Kaur, S. Saipriya, R. Singh, *AIP Conf. Proc.* **2015**, *1665*, 1.

[10] P. Yang, J. Wang, X. Zhao, J. Wang, Z. Hu, Q. Huang, L. Yang, *Appl. Phys. A: Mater. Sci. Process.* **2019**, *125*, 1.

[11] H. Lee, Y. T. Huang, M. W. Horn, S. P. Feng, *Sci. Rep.* **2018**, *8*, 1.

[12] P. K. Ooi, C. G. Ching, M. A. Ahmad, S. S. Ng, M. J. Abdullah, H. A. Hassan, Z. Hassan, *Sains Malays.* **2014**, *43*, 617.

[13] M. S. Jamal, S. A. Shahahmadi, P. Chelvanathan, H. F. Alharbi, M. R. Karim, M. Ahmad Dar, M. Luqman, N. H. Alharthi, Y. S. Al-Harthi, M. Aminuzzaman, N. Asim, K. Sopian, S. K. Tiong, N. Amin, M. Akhtaruzzaman, *Results Phys.* **2019**, *14*, 102360.

[14] V. Panneerselvam, K. K. Chinnakutti, S. Thankaraj Salammal, A. K. Soman, K. Parasuraman, V. Vishwakarma, V. Kanagasabai, *Appl. Nanosci.* **2018**, *8*, 1299.

[15] V. Figueiredo, E. Elangovan, G. Gonçalves, P. Barquinha, L. Pereira, N. Franco, E. Alves, R. Martins, E. Fortunato, *Appl. Surf. Sci.* **2008**, *254*, 3949.

[16] S. Bonomi, D. Marongiu, N. Sestu, M. Saba, M. Patrini, G. Bongiovanni, L. Malavasi, *Sci. Rep.* **2018**, *8*, 1.

[17] A. S. Subbiah, N. Mahuli, S. Agarwal, M. F. A. M. van Hest, S. K. Sarkar, *Energy Technol.* **2017**, *5*, 1800.

[18] H. J. Seok, A. Ali, J. H. Seo, H. H. Lee, N. E. Jung, Y. Yi, H. K. Kim, *Sci. Technol. Adv. Mater.* **2019**, *20*, 389.

[19] M. F. Nurfazliana, S. A. Kamaraddin, N. Nafarizal, H. Saim, M. Z. Sahdan, in *2014 IEEE Int. Conf. Semiconductor Electronics (ICSE2014)*, IEEE, Kuala Lumpur, Malaysia **2014**, pp. 100–103.

[20] S. Cho, *Met. Mater. Int.* **2013**, *19*, 1327.

[21] M. Gaidi, A. Hajjaji, M. Ali El Khakani, K. Kamimura, Z. Wang, Y. Onuma, S. Belhamri, N.-E. Hamdadou, *J. Phys.: Conf. Ser.* **2016**, *758*, 012007.

[22] F. N. Ajeel, A. Nazar Hussein, S. Khalaf Muhammad, S. Abdaul Mohsin, F. N. Ajeel, *J. Appl. Phys. Sci. Int.* **2015**, *4*, 178.

[23] J. Um, B. M. Roh, S. Kim, S. Eunkyung Kim, *Mater. Sci. Semicond. Process.* **2013**, *16*, 1679.

[24] Y. Ohya, S. Ito, T. Ban, Y. Takahashi, *Key Eng. Mater.* **2000**, *40*, 113.

[25] Z. Golshani, S. Maghsoudi, S. M. A. Hosseini, *Energy Rep.* **2022**, *8*, 13596.

[26] A. N. Hussain, K. I. Hassoon, M. A. Hassan, *J. Phys.: Conf. Ser.* **2020**, *1530*, 012140.

[27] D. S. Murali, S. Kumar, R. J. Choudhary, A. D. Wadikar, M. K. Jain, A. Subrahmanyam, *AIP Adv.* **2015**, *5*, 203502.

[28] D. Sivadas, S. Bhatia, P. R. Nair, *Appl. Phys. Lett.* **2021**, *119*, 203502.

[29] J. Dou, C. Zhu, H. Wang, Y. Han, S. Ma, X. Niu, N. Li, C. Shi, Z. Qiu, H. Zhou, Y. Bai, Q. Chen, *Adv. Mater.* **2021**, *33*, 2102947.

[30] N. W. Sangwaranatee, N. Sangwaranatee, M. Horprathum, C. Chananonnawathorn, M. Muntini, *Mater. Today: Proc.* **2018**, *5*, 15166.

[31] S. Das, T. L. Alford, *J. Appl. Phys.* **2013**, *113*, 244905.

[32] S. S. Shariffudin, S. S. Khalid, N. M. Sahat, M. S. P. Sarah, H. Hashim, *IOP Conf. Ser.: Mater. Sci. Eng.* **2015**, *99*, 012007.

[33] M. A. M. Patwary, C. Y. Ho, K. Saito, Q. Guo, K. M. Yu, W. Walukiewicz, T. Tanaka, *J. Appl. Phys.* **2020**, *127*, 085302.

[34] N. Serin, T. Serin, Ş. Horzum, Y. Çelik, *Semicond. Sci. Technol.* **2005**, *20*, 398.

[35] H. Çavuşoğlu, *Eur. J. Sci. Technol.* **2018**, *13*, 124.